

Progress in the Development of Solid-State Disk Laser^{a, b}

John Vetovec^c, Rashmi Shah, Tom Endo, Andrea Koumvakalis,
Kevin Masters, William Wooster, Kenneth Widen, and Steven Lassoovsky

Lasers & Electro-Optics Systems, The Boeing Company
6633 Canoga Avenue, Canoga Park, CA. 91309, USA

ABSTRACT

This work describes recent progress in the development of a solid-state disk laser that uses composite laser disks in active mirror configuration, edge-pumping, and cooling by microchannel-type heat exchanger. An innovative pressure clamping technique was used to mitigate thermo-mechanical distortions in the disk. A test article Yb:glass disk was operated at a thermal load corresponding to about 1 kW laser output in a steady-state regime with surface temperatures around 90°C while exhibiting less than $\lambda_{\text{Laser}}/10$ rms phase error. Measured pump uniformity approaching 90% validated the edge-pumping architecture.

Keywords: Solid-state laser, disk laser, active mirror, edge pumping, ytterbium, optical quality

1. INTRODUCTION AND BACKGROUND

Disk-type solid-state laser (SSL) is recognized for its inherently low susceptibility to thermo-optical distortions. This makes it suitable for large size, high-efficiency systems producing diffraction-limited beams (see e.g., [1]). Disk lasers in active mirror configurations have been built since 1960's [2] and are currently investigated in Germany [3] and in the U.S. at the Lawrence Livermore National Laboratory [4]. Recently, we reported the development of a new disk laser concept, known as the compact active mirror laser (CAMIL), which overcomes the limitations of prior concepts [5,6]. This work, describes the results of recent development testing project funded by DARPA.

CAMIL uses a large-aperture, edge-pumped laser gain medium disk mounted on a rigid, cooled substrate, Figures 1 and 2. The disk is of composite construction with a laser-active central portion and a perimetral edge. The disk material can be yttrium aluminum garnet (YAG), gadolinium gallium garnet (GGG), glass, or other host media. The central active portion of the disk (typically 2.5 mm in-thickness and 5 to 15 cm in-diameter) is doped with Nd or Yb ions. In our earlier work we have shown that the composite construction improves coupling between the pump diodes and the gain medium, aids concentration of pump radiation, provides cooling to the doped disk edge, and helps to suppress parasitic oscillations by absorbing or trapping amplified spontaneous emission (ASE) [7].

The substrate supporting the disk contains a built-in heat exchanger with microchannels on the front surface so that coolant can directly wet the back face of the laser disk. Except for the microchannels the front surface of the substrate is machined to optical flatness. The disk is attached to the substrate by a hydrostatic pressure differential between the surrounding atmosphere and the coolant fluid in the microchannels. This method of attachment is also known as "pressure clamping." This novel approach provides uniform cooling at high heat flux and effectively mitigates thermal deformations of the disk [8].

One key advantage of CAMIL is its scalability over a broad range of average laser powers. With each disk producing kilowatts of laser power, power scaling can be accomplished by changing the disk size and/or the number of disks in the laser. CAMIL can be used as a building block for construction of laser amplifiers and laser oscillators [9].

^a This effort was in-part funded by DARPA through AFOSR contract number F49620-02-C-0035

^b Distribution Statement A: Approved for Public Release, Distribution Unlimited (determined by DARPA on 03-29-2004)

^c jan.vetovec@boeing.com tel. (818) 586-3101, fax (818) 586-3074

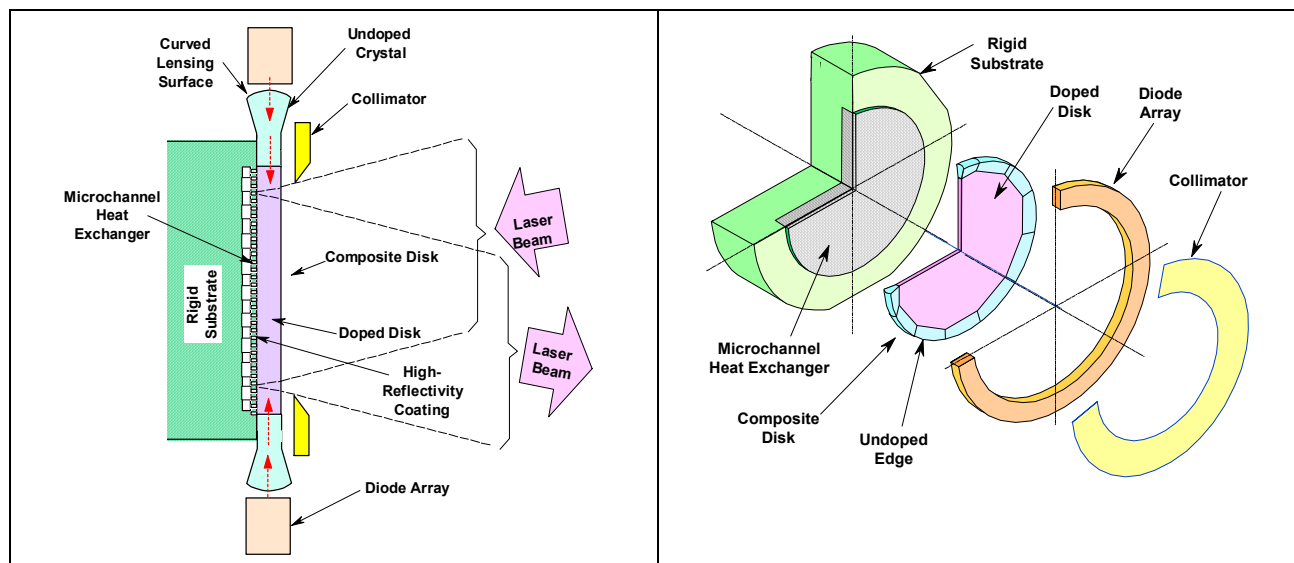


Figure 1: Edge-pumped CAMIL disk

Figure 2: Exploded view of edge-pumped CAMIL

2. DEVELOPMENT OF EDGE-PUMPED ARCHITECTURE

The key criteria for pump architecture in any SSL include 1) efficient transport of pump power to the gain medium, 2) efficient absorption of pump radiation, and 3) high uniformity of absorbed pump power density. In the edge-pumped disk, pump diode arrays are arranged around the circumference of the composite disk and generally point toward its center. Diode emitters are placed close to the perimetral edge of the composite disk to ensure good coupling efficiency into the material. Pump radiation is injected into the perimetral edge and is channeled into the central, laser-active portion of the disk where it is gradually absorbed [10]. Edge-pumping is very advantageous because it provides a long absorption path for the pump, which allows reduction of disk doping and makes it more practical to use laser ions with low absorption cross-sections.

Portions of the gain medium disk closer to the diodes are susceptible to being pumped more intensely than portions further away. Variations in deposition of pump energy can result in local heating, nonuniform gain, and loss of beam quality. Edge-pumped CAMIL exploits the natural divergence of pump diodes to achieve spatially uniform pumping. Beamlets produced by individual laser diode elements overlap inside the gain medium disk and their intensities are summed. Beamlet superposition can be balanced by absorption to produce a uniform pump distribution. Volumetric density of absorbed pump power at each point in the disk depends on the power output and divergence of individual diode elements, diode placement and pointing, and the density of absorbing ions in the gain medium.

The density profile of absorbed pump power in the edge-pumped disk was predicted by an analytic model outlined in our previous work [7]. Predicted profiles are evaluated in a statistical sense. Profile variations are described in the terms of standard deviation measured as a fraction of the root-mean-square (rms) value of absorbed power density. Note that profile uniformity $\equiv 1$ -variation. Parametric studies using this model revealed two approaches for diode placement that yield uniform pumping: a) fast axis parallel to the disk surface and b) fast axis perpendicular to disk surface, see Figure 3. In the former case (Figure 3a), uniform pump density distribution can be readily achieved with unlensed diode bars mounted on standard, water-cooled heat exchangers. However, this requires orienting the diode coolant manifolds parallel to the plane of the disk, which results in rather complicated coolant and electrical connections. In the latter case (Figure 3b), diode bars form a polygonal array with coolant manifolds perpendicular to the plane of the disk. This allows for simple coolant and electrical connections. One disadvantage of the latter approach is that the pump density distribution is more sensitive to diode arrangement, slow axis divergence, and disk doping.

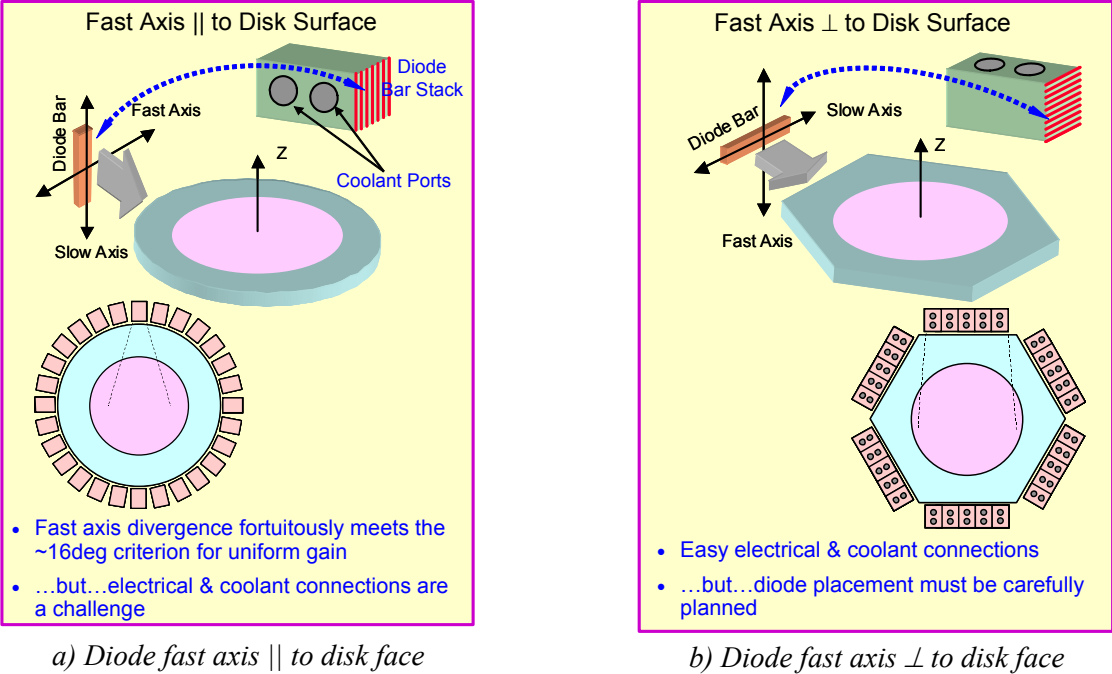


Figure 3: Two configurations of diode bars for edge pumping

To refine the polygonal configuration of diodes for this project we investigated hexagonal and octagonal diode arrangements. Figure 4 shows calculated variation of pump power density plotted against absorption scale length (x_L) for four cases of diode (slow axis) divergence in each hexagonal and octagonal array. It is evident that pump absorption over 90% and pump density variation 10% (i.e. uniformity 90%) can be obtained simultaneously in both cases. Figure 5 shows a segment of the edge-pumping architecture for octagonal array.

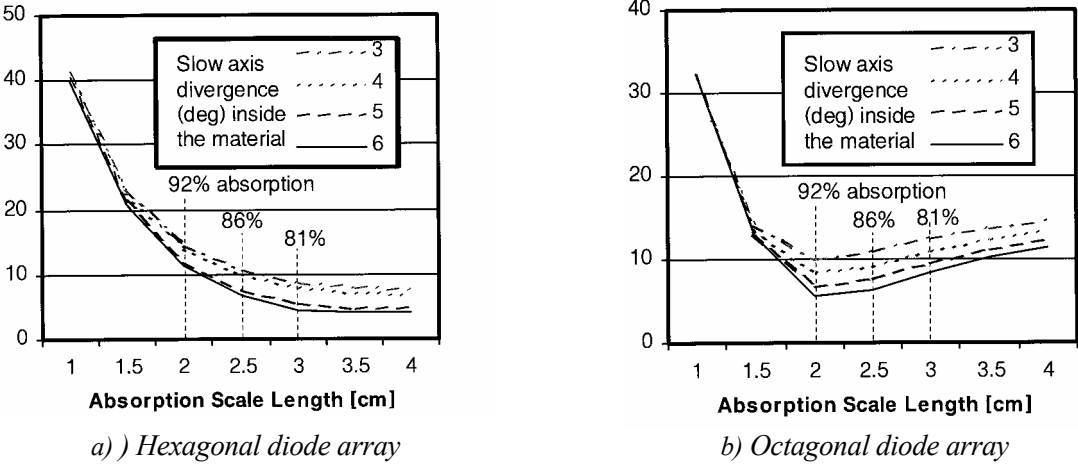


Figure 4: Variation of absorbed power density measured as a percentage of rms value versus absorption scale length for four cases of diode divergence in disks with hexagonal and octagonal diode arrays

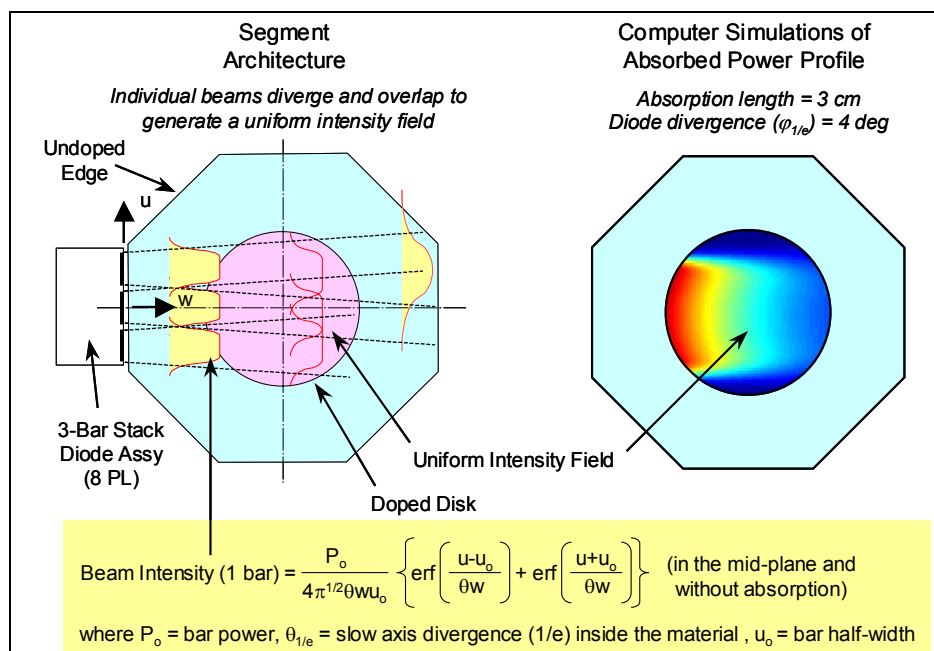


Figure 5: Edge-pump architecture using an octagonal diode array

3. COMPOSITE LASER DISK DESIGN AND FABRICATION

Crystals such as YAG and GGG offer much higher thermal conductivity than glass, which makes them often favored for construction of high-average power lasers. However, in CAMIL the relatively thin (2.5 mm) disk with a large cooled area also allows efficient use of glass despite its low thermal conductivity. Choosing glass has significant practical advantages because glass is inexpensive and is available in large sizes with optical quality superior to crystals. Finally, glass can be made athermal, which means that the coefficient of thermal expansion is balanced by negative dn/dt to make the coefficient of optical path essentially invariant with temperature.

The composite disk used in these tests comprised a central portion ($\text{Ø}5$ cm) doped with laser ions and a perimetral edge (10-cm octagon). The host material was Q-98 phosphate glass manufactured by Kigre, Inc. Ytterbium was selected for doping because of its small Stoke's shift and the resulting low heat fraction. In particular, when Yb is pumped at the zero-phonon line near 975 nm and lased at 1029 nm, its heat fraction is only about 5% of the absorbed pump power. Reduced heat load under these conditions makes glass even more attractive as the host material for the disk laser. The doping level for the test article disk was established to provide an absorption scale (e-folding) length of 2 cm at 941 nm. Since no prior data existed on Yb:Q-98, absorption cross-section was estimated based on similar materials.

Several techniques for fabricating the composite test article disks were considered including adhesive bonding, fusion bonding, low and high temperature diffusion bonding, sintering, and casting. Ultimately, the casting process was selected because it offered the prospects of high volume production of high-quality large-size composites at low cost. The composite Yb:glass billet was produced by Kigre, Inc. that is one of the few laser glass manufacturers in the world capable of producing large, laser-grade, optical quality glass composites. The production process involved several stages wherein a doped core billet several inches thick is cast first and a perimeter is cast into a form around it. After annealing, the billet is sliced with a diamond saw to yield several disks, Figure 6. Figure 7 shows one of the disks just prior to coating.

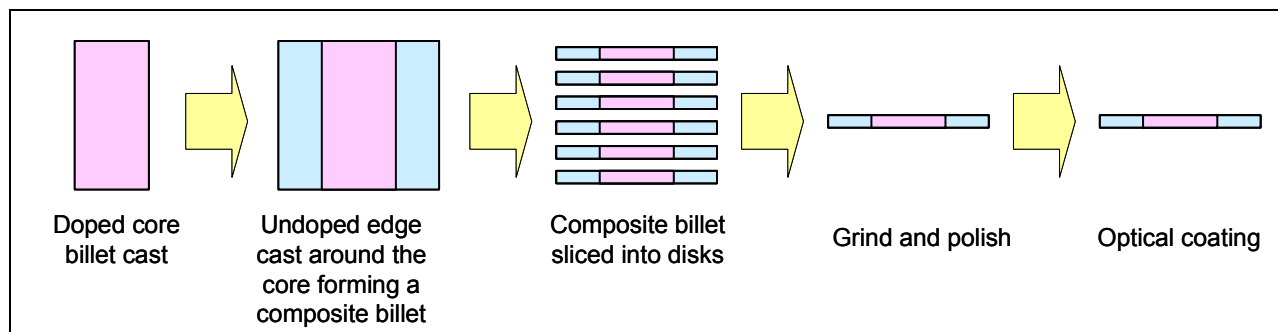


Figure 6: Key steps in fabrication of composite glass disks

4. HEAT EXCHANGER DESIGN AND FABRICATION

In CAMIL, the heat exchanger serves a dual purpose: 1) it removes waste heat from the disk and 2) provides a rigid substrate (strong back) to maintain the laser disk in an optically flat condition. The key requirements for the heat exchanger design include: handling the design heat flux, uniform heat removal, maintaining isothermal conditions on the back face of the disk, maintaining optical flatness, low coolant pressure drop, and economical flow rate. The heat exchanger uses open channels to allow direct wetting of the back surface of the disk by the coolant. The width of the open micro-channels was chosen to avoid excessive optical path difference due to local perturbation to isothermal surface [7]. Under nominal thermal load the back surface of the disk was predicted to be very isothermal with less than 1.3°C temperature peak-to-peak variations.

The heat exchanger was made of silicon because this material has a high thermal conductivity, high Young's modulus, low density, low coefficient of thermal expansion, commercial availability of suitable manufacturing processes, and traceability to full-scale hardware. The front surface of the heat exchanger was machined to optical flatness of $\lambda/20$ (@632 nm) to provide precision reference for the disk. Figure 8 shows the completed heat exchanger just prior to delivery.

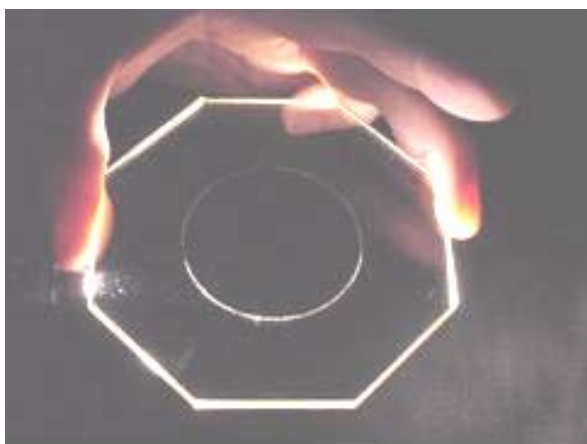


Figure 7: Composite laser disk sliced out of a production billet prior to coating

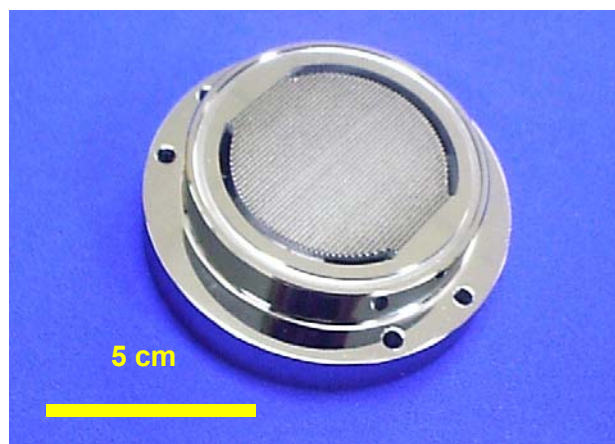


Figure 8: Completed heat exchanger

5. TEST SETUP AND TESTING

The composite disk was tested in a test cell pressurized to up to 100 psi to clamp the disk to the heat exchanger. An octagonal array of 24 diode bars each rated at 40 W of continuous output was used to inject up to 960 W of optical power at 941 nm into the perimetral edge of the disk. Figure 9 shows the arrangement of the diodes and the composite disk. The overall test setup is shown in Figure 10. Absorbed diode power pumped ytterbium ions into the 10624 cm^{-1} energy level in the ${}^2F_{5/2}$ manifold. Since no laser power was extracted, energy in the

upper laser level at 10327 cm^{-1} was radiated as spontaneous emission in vicinity of $1\text{ }\mu\text{m}$ wavelength. A significant portion of fluorescence power was trapped inside the disk. Because the ytterbium was operated below transparency, fluorescence absorbed by ground state ions became a significant contribution to the heat load in the central portion of the disk.

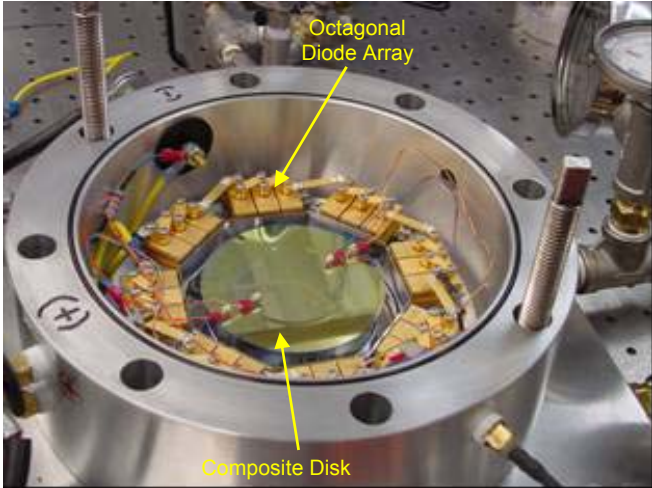


Figure 9: Composite test article disk installed on the heat exchanger

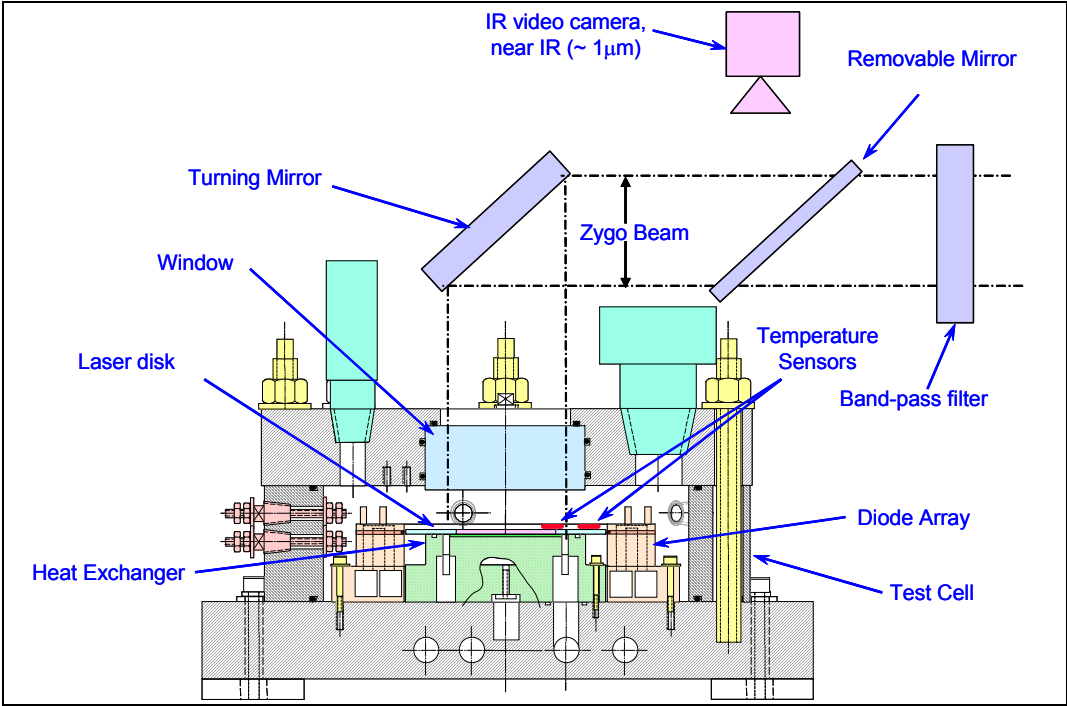


Figure 10: Test setup

The temperature of the front surface of the disk was measured using temperature sensors attached to the disk surface. An estimate of the volumetric heating rate in the doped portion of the disk was obtained by matching the measurements from temperature sensors to theoretical predictions from a 2-dimensional model. Figure 11 shows time variation of temperature (broken curve) measured in Test 471 and model predictions (solid curve) at matching volumetric heating rate. Note that starting from its “cold” condition the disk essentially reached a steady state “hot” condition in about 40 seconds.

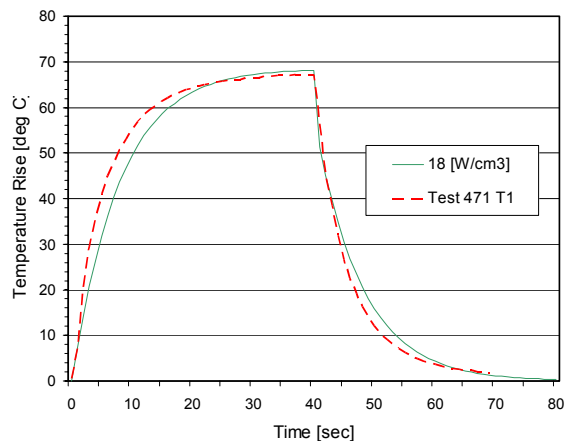


Figure 11: Temperature measurement in Test 471 (broken curves) vs. model predictions (solid curves)



Figure 12: IR fluorescence from the disk viewed by a broad band camera

Thermally driven distortions in the disk were measured interferometrically. An interferometer beam was directed into the test cell through the window in the top plate. The beam impinged on the test article laser disk, passed through the antireflective coating into the disk material, and was reflected from the high-reflectivity coating on its lower face. In this fashion, the interferometer beam made two passes through the disk material while detecting optical path difference (OPD) due to dn/dt , thermal expansion, and lifting of the disk from the heat exchanger. Fringe images from the interferometer were computer captured in a video format at up to 30 Hz, digitized, and processed off-line using FringeLab, a Boeing proprietary software. Figure 13 shows the time evolution of the phase error in Test 471. As the disk heats up to its steady state temperature, the phase error reaches its peak value of $0.18 \lambda_{632 \text{ nm}}$ rms phase error, which translates to about $\lambda_{\text{Laser}}/10$ rms.

Previous analysis using numerical models predicted that at high temperatures (around 100°C) and clamping pressure (differential) below 100 psi, the portion of the disk close to the junction between doped and undoped material would start lifting from the heat exchanger [9]. However, this effect was not detected in our tests. A possible explanation is offered by the Van der Waals forces acting between the optically flat surfaces of the disk and the heat exchanger. This suggests that the pressure clamping concept is more effective than originally anticipated.

The profile of absorbed pump power was obtained by viewing the disk fluorescence with an IR video camera that shared access to the disk with the interferometer. The IR camera signal was captured in video format, digitized and processed off-line using the MatLab[®] software package. After filtering out the high-frequency component, the variation of pump density was less than 12%, i.e., the pump uniformity was over 88%, Figure 14a. In a separate experiment the absorption scale length was measured at $x_L = 1.4$ cm, which was significantly less than the targeted 2 cm. This was due to the higher than expected absorption cross-section in the Q-98 glass. As seen in Figure 14b, power density profiles predicted by the model for $x_L = 1.4$ cm have a close correspondence to the measured profiles, thereby validating the edge-pumping model. If the doping in the disk is reduced to meet the original absorption goal ($x_L = 2$ cm) and minor adjustments are made to the diode pointing, the model predicts that the pump density variations in the octagonal configuration could be reduced to 4%, Figure 14c.

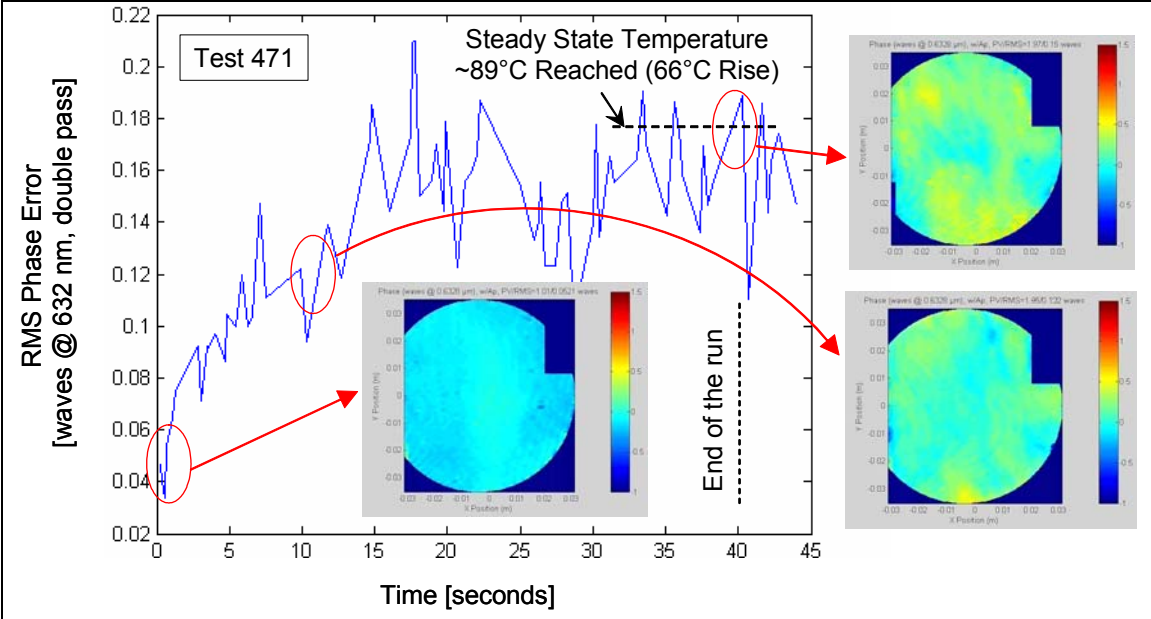


Figure 13: Time evolution of rms phase error in Test 471

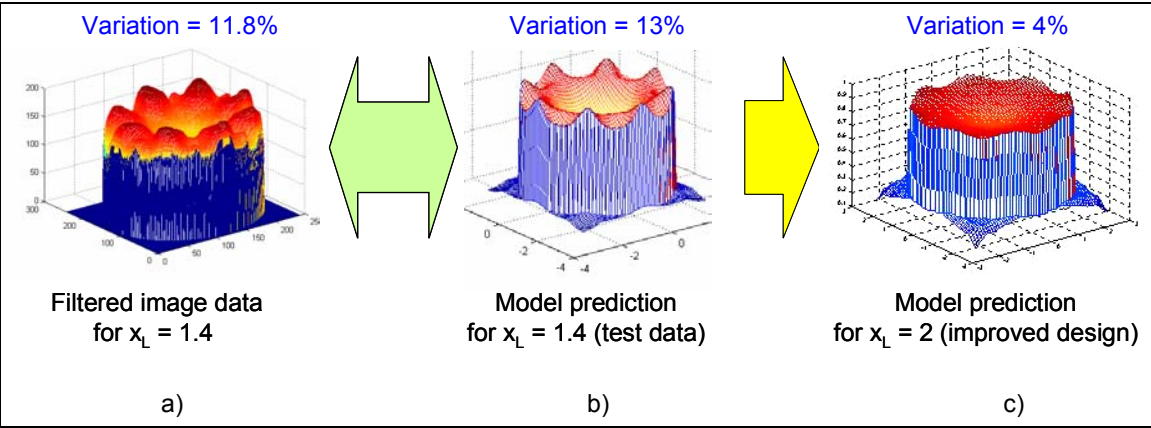


Figure 14: Comparison of absorbed power density distribution and model predictions

6. ENGINEERING CONCEPT

To achieve a very compact laser assembly, we developed a configuration with axisymmetric layout of the disks as shown in Figure 15. The number of components is reduced and assembly is simplified by mounting several CAMIL disks onto a common substrate containing internal heat exchangers and coolant manifolds. Two such substrates are positioned face-to-face on an optical bench [11]. Figure 16 shows an engineering concept reflecting this approach. The substrates are attached to a cylindrical optical bench that provides sufficient stiffness for maintaining optical alignment under operational dynamic loads. The assembly is further provided with power buses, and electric and fluid connections, and is then placed inside an enclosure protecting the components and maintaining the pressure required for disk attachment.

7. CONCLUSION

We presented an update on the development of a solid-state disk laser that uses composite laser disks in active mirror configuration, edge-pumping, and cooling by microchannel-type heat exchanger to overcome the limitations of prior designs. An innovative pressure clamping technique was used to mitigate thermo-mechanical distortions in the disk. Disk modules can be used as gain elements in a wide variety of laser

oscillator and power amplifier configurations. Such laser is very suitable for laser material processing requiring high-average power and high-brightness such as thick section cutting, deep-penetration welding, cutting and welding of aluminum in the manufacture of aircraft, and drilling of cooling holes in the manufacture of jet engines. Furthermore, 20- to 60-kW beams delivered through optical fibers are also required for thick section cutting in decontamination and decommissioning of nuclear power plants.

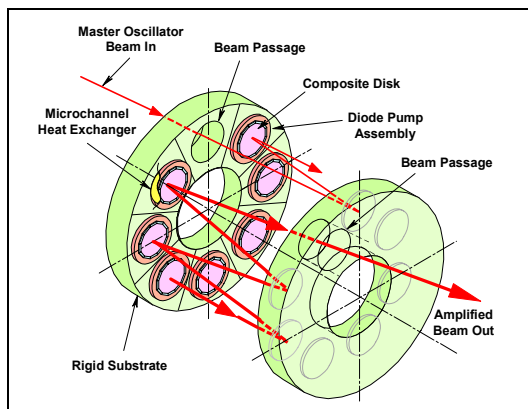


Figure 15: Axisymmetric layout showing multiple disks mounted on a common substrate

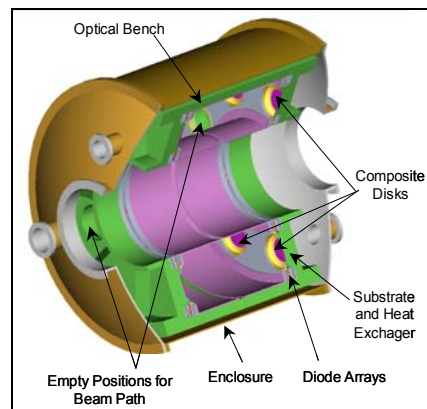


Figure 16: Engineering concept

ACKNOWLEDGEMENTS

The authors are indebted to Dr. Martin Stickley of DARPA for providing the project funds, counsel, and encouragement, and to AFOSR for managing the Boeing contract. They are also grateful to Drs. Charlie Turner Jr., Dennis Harris, John Stratton and Nicholas Koumvakalis of the Boeing Company; Dr. Georg Albrecht of the Lawrence Livermore National Laboratory; Dr. Paul Rudy of Coherent Inc.; Messrs. Tom Tonnessen and Jim Metz of InSync; Michael Myers of Kigre, Inc.; and Tom Thomas of TwinStar Optics for many useful discussions.

REFERENCES

1. W. Koechner, "Solid-state laser engineering," chapter 7: "Thermo-optic effects and heat removal," 5th edition, Springer-Verlag, New York, NY, 1999
2. D. C. Brown, J. H. Kelly, and J. A. Abate, "Active-mirror amplifiers: Progress and prospects," *IEEE J. of Quantum Electron.*, vol. 17, no. 9, 1755, 1981
3. Stewen, K. Contag, M. Larionov, A. Giesen, and H. Hugel, "1-kW CW thin disk laser," *IEEE J. Selected Topics in Quantum Electr.*, vol. 6, no. 4, pp. 650-657, July/August 2000
4. L. Zapata, R. Beach and S. Payne, "Composite thin-disk laser scalable to 100 kW average power output and beyond", in the Technical Digest from the Solid State and Diode Laser Technology Review, held in Albuquerque, NM., June 5-8, 2000
5. J. Vetrovec, "Active mirror amplifier for high-average power," SPIE vol. 4270 (2001)
6. J. Vetrovec, "Compact active mirror laser-CAMIL," SPIE vol. 4630 (2002)
7. J. Vetrovec, R. Shah, T. Endo, and A. Koumvakalis., "Development of Solid-State Disk Laser for High-Average Power," SPIE vol. 4968 (2003)
8. J. Vetrovec, US Patent No. 6,339,605
9. J. Vetrovec, "Ultrahigh-average power solid-state laser," SPIE vol. 4760 (2002)
10. J. Vetrovec, US Patent No. 6,625,193
11. J. Vetrovec, US Patent No. 6,603,793